OUROBOROS is a master regulator of the gametophyte to sporophyte life cycle transition in the brown alga Ectocarpus

Susana M. Coelho, Olivier Godfroy, Alok Arun, Gildas Le Corguillé, Akira F. Peters, J. Mark Cock

OUROBOROS is a master regulator of the gametophyte to sporophyte life cycle transition in the brown alga *Ectocarpus*

Susana M. Coelho[a,b], Olivier Godfroy[a,b], Alok Arun[a,b], Gildas Le Corguillé[c], Akira F. Peters[d], and J. Mark Cock[a,b,1]

[a]Centre National de la Recherche Scientifique, Unité Mixte de Recherche 7139, Laboratoire International Associé Dispersal and Adaptation in Marine Species, Station Biologique de Roscoff, 29682 Roscoff Cedex, France; [b]Université Pierre et Marie Curie, Université Paris 6, Marine Plants and Biomolecules Laboratory, Unité Mixte de Recherche 7139, Station Biologique de Roscoff, 29682 Roscoff Cedex, France; [c]Service Informatique et Génomique, Station Biologique de Roscoff, 29682 Roscoff Cedex, France; and [d]Bezhin Rosko, 29250 Santec, France

Edited by Diter von Wettstein, Washington State University, Pullman, WA, and approved May 31, 2011 (received for review February 25, 2011)

The brown alga *Ectocarpus siliculosus* has a haploid–diploid life cycle that involves an alternation between two distinct generations, the sporophyte and the gametophyte. We describe a mutant, *ouroboros* (*oro*), in which the sporophyte generation is converted into a functional, gamete-producing gametophyte. The life history of the mutant thus consists of a continuous reiteration of the gametophyte generation. The *oro* mutant exhibited morphological features typical of the gametophyte generation and accumulated transcripts of gametophyte generation marker genes. Genetic analysis showed that *oro* behaved as a single, recessive, Mendelian locus that was unlinked to the *IMMEDIATE UPRIGHT* locus, which has been shown to be necessary for full expression of the sporophyte developmental program. The data presented here indicate that *ORO* is a master regulator of the gametophyte-to-sporophyte life cycle transition and, moreover, that *oro* represents a unique class of homeotic mutation that results in switching between two developmental programs that operate at the level of the whole organism.

brown algae | development | phaeophyceae | stramenopiles

Many organisms have life histories that involve alternation between two multicellular generations, a sporophyte and a gametophyte (1). A considerable amount of theoretical work has been carried out to understand the evolutionary and ecological significance of such complex life cycles (1). Haploid–diploid life cycles (i.e., cycles in which there is an alternation between a diploid sporophyte and a haploid gametophyte generation) pose a particular problem because it is necessary to explain why they do not evolve towards either haploid or diploid life cycles, both of which have theoretical advantages under some conditions. Possible advantages specific to haploid–diploid life cycles include the potential of the two generations to exploit alternative ecological niches, avoidance of biotic aggressors (because of differential susceptibility of the two generations), and a reduced cost of sex (one meiosis/fertilization every two generations). However, very little experimental work has been carried out to test these various hypotheses (1, 2). One of the limiting factors in this regard is that the mechanisms that regulate life cycle progression at the molecular level remain poorly understood.

Variant life cycles could potentially provide insight into underlying regulatory mechanisms. In a normal haploid–diploid life cycle, the two generations are demarcated by meiosis, which produces the spores that will become the gametophyte generation, and gamete fusion, which produces the zygote that will become the sporophyte generation. However, many species exhibit various forms of apomixis, in which the life cycle progresses without the occurrence of meiosis or fertilization (3, 4). Apomictic life cycles can involve both apospory (formation of a gametophyte from a sporophyte without meiosis) and apogamy (formation of a sporophyte by parthenogenesis of a gametophyte cell). Genetic analysis of apomictic systems is complicated by a number of factors (5), but the existence of these systems does suggest that life cycle regulation may be amenable to genetic analysis. This contention has been supported by experimental work on the non-apomictic species *Arabidopsis thaliana* and on non-apomictic strains of *Physcomitrella patens*, in which phenomena associated with apomixis, such as parthenogenesis, have been observed in mutant strains.

Arabidopsis strains carrying mutations in homologs of PRC2 polycomb complex component genes or in the *RETINOBLASTOMA-RELATED* gene, a regulator of the PRC2 complex, exhibit fertilization-independent development of the endosperm and, in some cases (*FERTILIZATION INDEPENDENT ENDOSPERM1*/*MEDEA*, *FERTILIZATION INDEPENDENT ENDOSPERM2*, and *MULTICOPY SUPPRESSOR OF IRA 1 [MSI1]* mutants), parthenogenetic development of embryo-like structures (6–11). These embryo-like structures usually abort after undergoing a few cell divisions, making it difficult to determine definitively whether the structure formed corresponds to a bona fide embryo. However, strong evidence for a switch from the gametophyte to the sporophyte developmental program has been obtained for the *MSI1* mutant by analyzing the expression of sporophyte generation marker genes in the embryo-like structure (12). Together, these observations suggest that the PRC2 complex acts to prevent transitions from the gametophyte to the sporophyte developmental program in the *Arabidopsis* gametophyte, acting as part of a developmental switch for this life cycle transition. Similar observations have been made in the moss *P. patens*, where mutations in either the *PHYSCOMITRELLA PATENS CURLY LEAF* (*PpCLF*) or the *PHYSCOMITRELLA PATENS FERTILIZATION INDEPENDENT ENDOSPERM* genes (both of which are predicted to encode components of a PRC2 complex) result in fertilization-independent production of a sporophyte-like body on side branches of the gametophytic protonema filaments (13, 14). In both studies, sporophyte marker genes were used to verify that the structures produced corresponded to the sporophyte generation. As in *Arabidopsis*, sporophyte development arrests prematurely. Arrest occurs partly because an active PRC2 complex seems to be needed for a later transition within the sporophyte, from the vegetative to the reproductive phase (production of the sporangium). However, even restoration of *PpCLF* expression at this later stage was not sufficient to produce a functional sporophyte, suggesting either that the sporophyte generation also depends on a factor supplied by the underlying gametophore (on which it normally grows) or that the haploid nature of the structure prevents full sporophyte development. Similar factors may explain the abortion of fertilization-independent embryos in *Arabidopsis* mutants. In this respect, brown

Author contributions: S.M.C. and J.M.C. designed research; S.M.C., O.G., A.A., A.F.P., and J.M.C. performed research; S.M.C., O.G., A.A., G.L.C., and J.M.C. analyzed data; and S.M.C. and J.M.C. wrote the paper.

The authors declare no conflict of interest.

This article is a PNAS Direct Submission.

Data deposition: The data reported in this paper have been deposited in the ArrayExpress database, http://www.ebi.ac.uk/arrayexpress/ (accession no. E-MTAB-485).

[1]To whom correspondence should be addressed. E-mail: cock@sb-roscoff.fr.

This article contains supporting information online at www.pnas.org/lookup/suppl/doi:10.1073/pnas.1102274108/-/DCSupplemental.

macroalgae represent interesting alternative model systems to study the alternation of generations in haploid–diploid life cycles because they can exhibit a remarkable plasticity with regard to ploidy and because, in species with haploid–diploid life cycles, the two generations of the life cycle often develop completely independently, after the release of single-cell propagules into the surrounding seawater.

The filamentous alga *Ectocarpus siliculosus* (Dillwyn) Lyngbye is an emerging model for the brown algae (15), and a number of molecular and genetic tools have recently been made available, including a complete genome sequence (16, 17). *Ectocarpus* has a haploid–diploid life cycle involving alternation between two independent heteromorphic generations, the sporophyte and the gametophyte (Fig. S1*A*). In addition, unfused gametes can develop parthenogenetically to produce partheno-sporophytes. One experimental advantage of this parthenogenesis is that mutations affecting sporophyte development are directly expressed phenotypically in haploid partheno-sporophytes, facilitating mutant screens (18). A spontaneous mutation (*immediate upright*; *imm*), in which the sporophyte generation exhibits several characteristics of the gametophyte, including an asymmetric initial cell division and absence of a basal system of prostrate filaments, has recently been described (18). Here we characterize a second *Ectocarpus* life cycle mutant, *ouroboros* (*oro*), which exhibits homeotic conversion of the sporophyte generation into a fully functional gametophyte. The *oro* mutation represents a unique class of homeotic mutation, causing switching between two different developmental programs that operate at the level of the whole organism.

Results

***ouroboros* Mutant Parthenotes Closely Resemble Wild-Type Gametophytes.** The *oro* mutant was isolated after UV mutagenesis of freshly released gametes of *Ectocarpus* strain Ec 32. In contrast to the situation in wild-type *Ectocarpus*, where gametes germinate parthenogenetically (i.e., in the absence of gamete fusion) to produce partheno-sporophytes (Fig. S1*A*), parthenotes of the *oro* mutant exhibited both morphological and functional features typical of gametophytes. The first cell division was asymmetrical, rather than being symmetrical as in the wild-type partheno-sporophyte (18), resulting in cells with rhizoid and upright filament identities (Fig. 1 *A*–*C*). Mutant individuals produced richly branched thalli, again typical of the gametophyte, which lacked the prostrate basal system found in the sporophyte (Fig. 1 *D*–*F*). Plurilocular sexual organs formed after 3 wk in culture and resembled gametangia rather than sporangia, having an elongated shape and never occurring at the tips of the upright filaments (Fig. 1 *G*–*I*). Furthermore, *oro* parthenotes never produced unilocular sporangia, a feature that has been observed only during the sporophyte generation.

Many *oro* parthenotes were indistinguishable from wild-type gametophytes throughout their development, but minor differences were observed for some *oro* individuals during early development. For example, wild-type sporophytes produce a base consisting of round cells strongly adhering to the substratum, whereas gametophytes tend to float off into the medium (18). Some *oro* individuals exhibited weak adherence to the substratum and produced a small number of round cells during the early stages of development (Fig. 1*J*). However, these sporophyte-like features were only observed transiently. When 45 parthenotes that exhibited this intermediate phenotype were isolated and their development was monitored, all developed gametophyte morphology within 6 d (Fig. 1*K*). Zoids released by the plurilocular organs of the *oro* mutant germinated to produce individuals that reiterated the *oro* phenotype (Fig. S1*B*). Transmission of the phenotype by this asexual pathway occurred stably for at least 36 asexual generations, and the phenotype was not affected by cultivation at 5, 10, or 20 °C or under different daylength regimes.

To further investigate the nature of the *oro* parthenotes, we developed a simple staining technique to distinguish between the sporophyte and gametophyte generations. The carbohydrate binding dye Congo red, which is used to stain xylan fibers in algal cell walls (19), stained the gametophyte, but not the sporophyte,

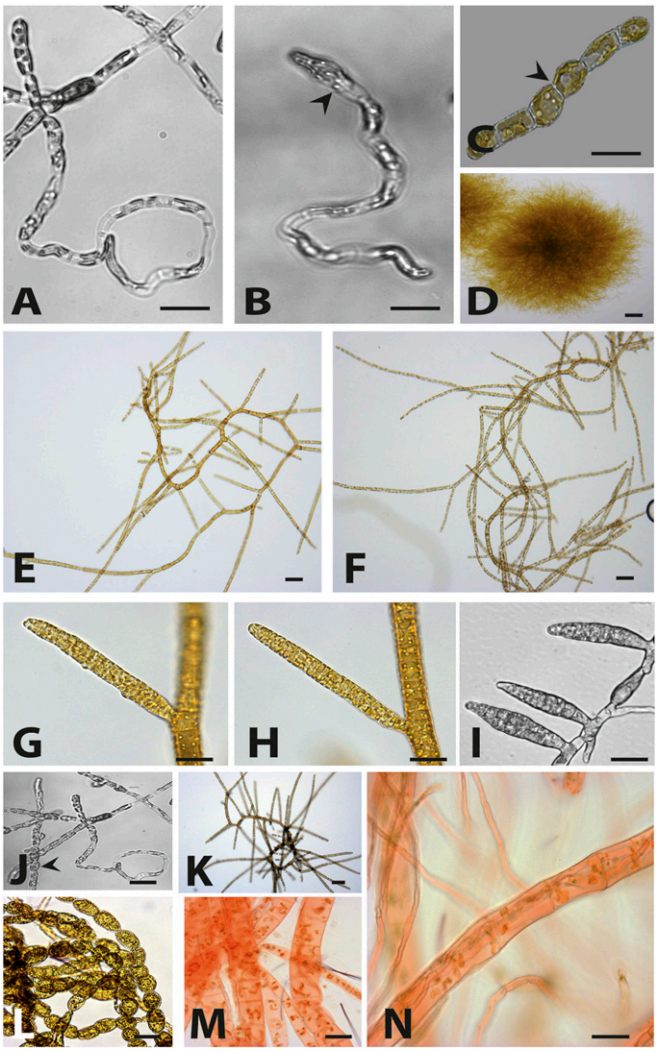

Fig. 1. *oro* mutant parthenotes closely resemble wild-type gametophytes. Representative images are shown. (*A*) Wild-type gametophyte germling (4 d old). (*B*) *oro* parthenote germling (4 d old). Note the asymmetrical first cell division (arrowhead). (*C*) Wild-type partheno-sporophyte germling (2 d old). Note the symmetrical first cell division (arrowhead). (*D*) Adult wild-type sporophyte (3 wk old). (*E*) Adult wild-type gametophyte (3 wk old). (*F*) Adult *oro* parthenote (3 wk old). (*G*) Plurilocular gametangium of a wild-type gametophyte. (*H*) Plurilocular gametangium of an *oro* parthenote. (*I*) Plurilocular sporangia of a wild-type partheno-sporophyte. (*J*) Round cells present during the early development of a few *oro* individuals (arrowhead). (*K*) *oro* individuals that had round cells during early development reverted to gametophyte morphology. (*L*) Wild-type partheno-sporophytes stained with Congo red (no red staining). (*M*) Wild-type gametophytes stained with Congo red (showing the characteristic red color). (*N*) *oro* individuals are Congo red positive. (Scale bars: 10 μm.)

of wild-type *Ectocarpus* (Fig. 1 *L* and *M*). The *oro* parthenotes were stained by Congo red, which again indicates that these individuals are gametophytes (Fig. 1*N*). Wild-type sporophytes and gametophytes also differ in their response to unidirectional light during early development, with gametophytes exhibiting a significantly more marked response to this stimulus (18). Approximately 90% of the *oro* parthenotes germinated away from unidirectional light (Fig. S2). This result was not significantly different from that obtained for a wild-type gametophyte (χ^2 = 1.46, $P > 0.05$, df = 1, n = 305) but was significantly different from that obtained with wild-type partheno-sporophytes (χ^2 = 29.60, $P < 0.001$, df 1, n = 1,030). An analysis of marker genes whose transcripts have been shown to exhibit significantly dif-

ferent levels of abundance during the two generations of the life cycle (18) showed that *oro* parthenotes accumulated transcripts that had been shown to be significantly more abundant in the gametophyte generation and, conversely, had reduced levels of transcripts that had been shown to be significantly more abundant in the sporophyte (Fig. 2).

***oro* Is a Single-Locus, Recessive Mutation That Causes Conversion of the Sporophyte into a Functional Gametophyte.** Zoids released from the plurilocular sexual organs of the male *oro* mutant fused with female gametes from the wild-type strain Ec 25 in crossing experiments to produce zygotes, indicating that the *oro* zoids were gametes and not spores (Fig. S3*A*). This result demonstrated that the *oro* parthenotes not only exhibit gametophyte morphology but are actually functional gametophytes.

Three of the zygotes from the cross between the *oro* mutant and Ec 25 were raised to maturity. All three individuals exhibited a typical sporophyte pattern of growth throughout their development and produced unilocular sporangia, indicating that the *oro* mutation was recessive (Fig. S3*B*). Sporophyte progeny were also obtained when the *oro* mutant was crossed with another, more distantly genetically related strain, Ec 568 (20).

To analyze the genetic inheritance of the *oro* locus, 14 unilocular sporangia were isolated individually from 3 diploid sporophytes derived from the cross between the *oro* mutant and the female strain Ec 25. These sporangia, which each contained >100 meiospores (derived from a single meiosis followed by at least five mitotic divisions), produced 14 meiotic "families" of gametophytes, all of which exhibited a germination pattern typical of wild-type gametophytes. Therefore, there was no evidence that the *oro* mutation had a phenotypic effect during the gametophyte generation, which was to be expected if the effect of the mutation is to convert the sporophyte into a gametophyte. For each of the families derived from a single unilocular sporangium, between 19 and 27 gametophytes were sub-isolated. Gametes produced by these gametophytes were allowed to germinate parthenogenetically, and the pattern of growth of the parthenotes was monitored (Table S1). Overall, 162 gametophytes produced parthenotes that developed as partheno-sporophytes (as expected for wild-type individuals), and 177 produced parthenotes with the *oro* phenotype. These figures are consistent with a 1:1 segregation ratio and Mendelian inheritance of a single-locus recessive mutation (ANOVA, $F_{1,26} = 1.07$, $P = 0.3$). The sex of several individuals each from 12 of the unilocular-sporangium-derived families that exhibited an *oro* phenotype was determined in test crosses with male and female tester strains: 33 of the *oro* plants tested were females, and 48 were males (Table S2). These data indicated that the *ORO* locus was not linked to the sex locus (ANOVA, $F_{1,22} = 3.21$, $P = 0.09$).

Diploid Individuals That Are Homozygous for the *oro* Mutation Exhibit a Gametophyte Phenotype. To determine whether diploid sporophytes (produced by the fusion of two gametes) were also converted to gametophytes in the presence of the *oro* mutation, a female *oro* strain (generated by the segregation analysis described above) was back-crossed with the male *oro* strain. The diploid progeny of this cross exhibited a similar phenotype to *oro* parthenotes except that the conversion to gametophyte morphology was slightly less marked. Many round cells (typical of sporophytes) could be observed during early development, but, as had been observed with the parthenotes, gametophyte morphology was adopted as growth progressed. Crosses ($n = 11$) with female (Ec 25 and Ec 410) and male (Ec 400 and Ec 32) tester strains demonstrated that the *oro* homozygous individuals produced functional gametes and that these gametes behaved as males, despite the presence of both the male and female haplotypes of the sex locus.

Genetic Interactions Between the *oro* and *imm* Mutations. Individuals carrying both the *oro* and the *imm* mutations were constructed by crossing *imm* strain Ec 419 and *oro* strain Ec 494. All 14 of the

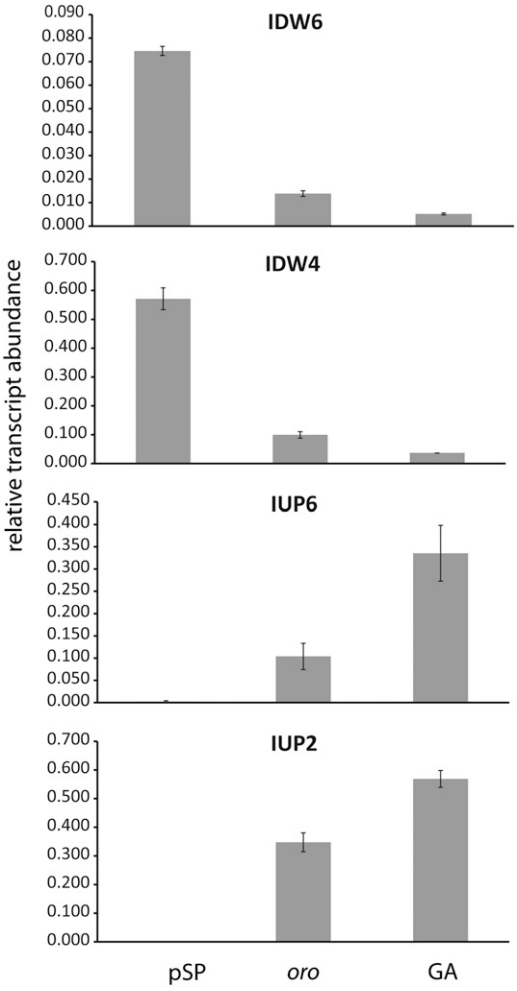

Fig. 2. qRT-PCR analysis of the abundances of gene transcripts in the *oro* mutant compared with wild-type gametophyte (GA) and partheno-sporophyte (pSP). The abundance of transcripts of four genes that have been shown to be differentially expressed in the gametophyte and sporophyte generations (18) was assayed in *oro* individuals. Data are means of three independent biological replicates ± SE. Transcript abundance was significantly different in the *oro* and GA samples compared with the wild-type pSP sample for all of the genes tested (ANOVA, $P < 0.05$). (From top to bottom) *IDW6*, Esi0351_0007; *IDW4*, Esi0085_0048; *IUP6*, Esi0031_0170; *IUP2*, Esi0416_0001.

zygotes isolated from this cross developed as wild-type sporophytes, indicating that complementation had occurred. Sixteen unilocular sporangia were isolated from one of the sporophytes (Ec 560), and between 9–20 gametophytes were sub-isolated from each of the meiotic families derived each from a single unilocular sporangium. Parthenotes that developed from gametes produced by these gametophytes exhibited one of four different patterns of early development (Table S3 and Fig. 3 *A–E*): (*a*) individuals morphologically identical to the wild-type partheno-sporophyte; (*b*) immediate development of erect filaments and production of a straight, rather than wavy, rhizoid (the phenotype of the *imm* mutant; ref. 18); (*c*) parthenotes with the phenotype described above for the *oro* mutant, i.e., gametophyte-like but with the formation of a small number of round cells during early development in some individuals; and (*d*) parthenotes that more strongly resembled the gametophyte during early development (absence of round cells) except that some individuals possessed a straight rather than wavy rhizoid. For the phenotypic classes *c* and *d*, all individuals rapidly adopted a typical gametophyte morphology as they developed (Fig. 3*F*). At maturity, parthenotes of classes *a* and *b* were functional sporophytes (producing unilocular sporangia

and plurilocular sporangia releasing mitospores and not gametes), whereas parthenotes of classes *c* and *d* were functional gametophytes, producing gametes that were able to fuse with gametes of the opposite sex. These phenotypic data indicated that the four classes corresponded to the following genotypes: (*a*) *IMM ORO*, (*b*) *imm ORO*, (*c*) *IMM oro*, and (*d*) *imm oro*. The four different phenotypic groups occurred in equal proportions (ANOVA, $F_{3,60} = 0.83$, $P = 0.5$). Note that the three mutant classes exhibited gametophyte-like phenotypic features to an increasing degree as follows: *imm* < *oro* < *imm oro*. All of the phenotypic classes were stable for at least eight asexual generations (asexual propagation being via mitospores in the case of classes *a* and *b* and via parthenogenetic development of gametes in the case of classes *c* and *d*).

To confirm that parthenotes of class *d* corresponded to *imm oro* double mutants, one individual from this class was crossed with a wild-type strain (Ec 32). Seven sporophytes with wild-type phenotypes were derived from this cross, and 15–25 gametophytes were produced from each sporophyte. Phenotypic analysis of the parthenotes derived from these gametophytes confirmed that the original individual carried both the *imm* and *oro* mutations (Table S4).

Comparison of mRNA Abundances in Life Cycle Mutants with the Wild-Type Sporophyte and Gametophyte. An expressed-sequence-tag-based microarray carrying probes corresponding to 10,600 of the 16,256 genes identified in the *Ectocarpus* genome (16, 21) was used to carry out a broad analysis of changes in steady-state mRNA abundances in the life cycle mutants (ArrayExpress accession no. E-MTAB-485). Transcript abundances were compared in parthenotes of all four possible classes of segregant in the population derived from the cross between the *imm* and *oro* mutants: (*a*) *IMM ORO* (wild-type partheno-sporophyte), (*b*) *imm ORO*, (*c*) *IMM oro*, and (*d*) *imm oro* individuals, using bulked segregants to minimize variance due to unlinked loci. A fifth sample corresponding to the wild-type gametophyte was also analyzed to provide a reference for the gametophyte generation of the life cycle. We carried out pairwise comparisons of each of the three mutant samples and the gametophyte sample with the wild-type partheno-sporophyte sample using the Significance Analysis of Microarrays (SAM) method (22). In each case, the genes for which we detected significant changes in mRNA abundance were assigned to a broad range of Gene Ontology (GO) categories (Dataset S1). This result indicated that both the *imm* and the *oro* mutations lead to complex modifications of cellular mRNA levels, involving changes in the expression levels of genes with roles in many different cellular processes. A GO slim analysis (http://www.geneontology.org) was carried out to look for general trends across the four different comparisons. Only one GO slim category, "protein metabolic process" (GO:
0019538), was represented solely in samples that contained functional gametophytes (*oro* mutant, *imm oro* double mutant, and wild-type gametophyte).

Fig. 4 illustrates the overlaps between the lists of differentially expressed genes identified in the four comparisons (*imm, oro*, and *imm oro* mutant strains and wild-type gametophyte with partheno-sporophyte). In all four comparisons, more genes were identified as being up-regulated than down-regulated (between 3- and 62-fold difference). This result suggests that the transition from the sporophyte to the gametophyte stage involves primarily gene induction rather than gene repression.

To carry out a broad cluster analysis, a set of 4,046 genes that exhibited significant changes in transcript abundance across the five samples analyzed in the microarray experiment were identified by applying a one-way ANOVA test. The 4,046 genes could be grouped into four clusters (Fig. S4*A*). The two largest clusters corresponded to genes whose transcripts tended to exhibit abundances in the mutant samples that were intermediate between those in the wild-type sporophyte and gametophyte samples, with preferential expression either in the sporophyte (cluster 1) or in the gametophyte (cluster 2). These expression patterns were consistent with intermediate phenotypes exhibited by the single- and double-mutant lines. A GO slim analysis indicated that GO categories associated with primary metabolism, including carbohydrate and lipid metabolism, and related functions such as transport were overrepresented in cluster 1 and underrepresented in cluster 2. In contrast, GO categories associated with protein synthesis and modification and other basic cellular processes, such as cell cycle, DNA replication, and developmental processes, showed the opposite trend (Fig. S4*B*). These trends indicate that there may be differences in the allocation of cellular resources in the two generations, perhaps

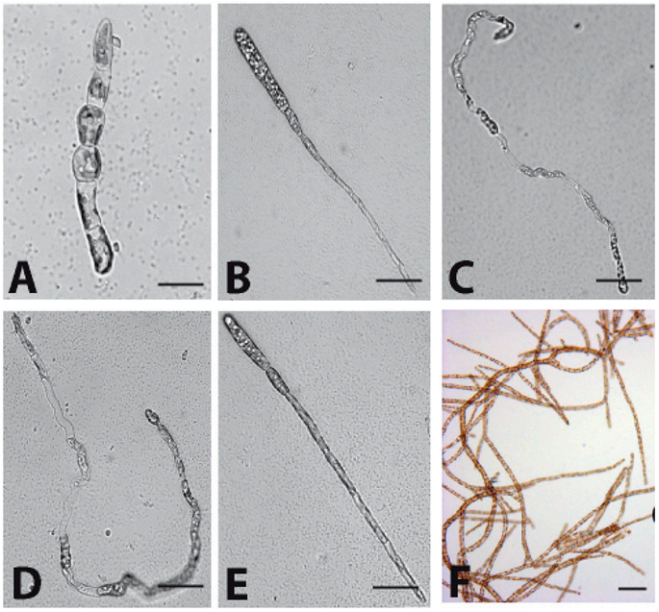

Fig. 3. Segregation analysis of the *oro* and *imm* loci. (*A*) Germling showing a wild-type partheno-sporophyte phenotype. (*B*) Germling showing an *imm* phenotype. (*C*) Germling showing an *oro* phenotype. (*D* and *E*) Germlings showing *imm oro* double-mutant phenotypes. (*F*) *imm*-like germlings from the *imm oro* mutants develop into gametophytes. See text for details. (Scale bars: 10 μm.)

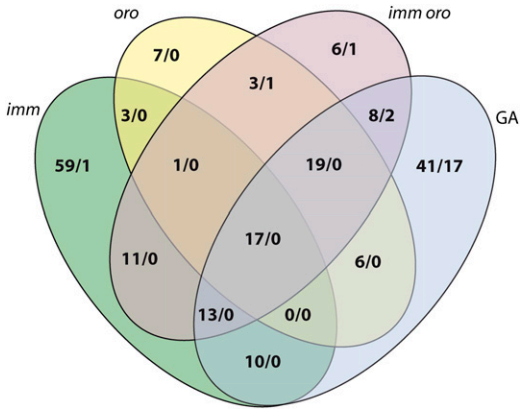

Fig. 4. Venn diagram showing the overlap between the sets of genes that had significantly different transcript abundances in the mutant (*imm, oro, imm oro*) strains and in the wild-type gametophyte (GA) compared with the wild-type partheno-sporophyte. The two numbers separated by a slash indicate the number of genes whose transcripts were significantly more (to the left) or less (to the right) abundant in the indicated sample, compared with the wild-type partheno-sporophyte.

associated with adaptation to different ecological niches or growth habits.

Quantitative RT-PCR (qRT-PCR) Analysis of Gene Expression. In an effort to better understand the molecular mechanisms underlying the alternation between the sporophyte and gametophyte generations, we searched the microarray data for genes that were differentially expressed in mutant and wild-type samples and that were predicted to encode proteins with potentially interesting functions (regulatory proteins, for example). Nine genes were selected, to which we added the *Ectocarpus ARGONAUT1* gene because there is accumulating evidence that small RNA pathways play important roles at key stages of the life cycle (23, 24). Transcript abundances for these 10 genes were then assayed by using qRT-PCR in five samples corresponding to those analyzed in the microarray experiment (Fig. 5 and Table S5). Transcripts of 9 of the genes analyzed exhibited either increases (Esi0308_0025, Esi0556_0008, Esi0074_0057, Esi0049_0053, Esi0009_0052) or decreases (Esi0095_0057, Esi0203_0032, Esi0245_0009, Esi0292_0018) in abundance in both the wild-type gametophyte sample and in some or all of the mutant samples, suggesting that these are life cycle-regulated genes that are influenced by the *imm* and/or the *oro* loci. The proteins encoded by these genes include a putative transcription factor (Esi0095_0057) and the ARGONAUT1 protein (Esi0203_0032). Interestingly, the gradual increases in the abundances of the Esi0308_0025 (predicted to encode a serine/threonine kinase) and Esi0074_0057 (predicted to encode a Homeodomain-like protein) transcripts when the *imm*, *oro*, *imm oro*, and wild-type gametophyte samples were compared correlated with the increasingly gametophyte-like nature of the individuals in each of these samples that was observed during the morphological analysis described above. Moreover, for Esi0308_0025, there was a synergistic effect of the *imm* and *oro* mutations resulting in a greater increase in transcript abundance in the *imm oro* double mutant than with either of the individual mutations alone. The Esi0556_0008 transcript increased in abundance only in the samples that contained functional gametophytes (wild-type gametophyte, *oro* mutant, and *imm oro* double mutant), suggesting that this gene may be important for the transition from sporophyte to gametophyte function rather than, for example, for a morphological feature of the gametophyte that is not directly related to life cycle function. Esi0556_0008 is predicted to encode an extracellular structural protein. For Esi0068_0016, there was no obvious correlation between transcript levels in the mutant lines and in the wild-type gametophyte. This result was consistent with the data from the microarray analysis, which suggested that the mutations do not exactly reproduce the phenotype of the wild-type gametophyte, even in the case of the *imm oro* double mutant, which is a functional gametophyte with morphological characteristics that are almost identical to those of the wild-type gametophyte.

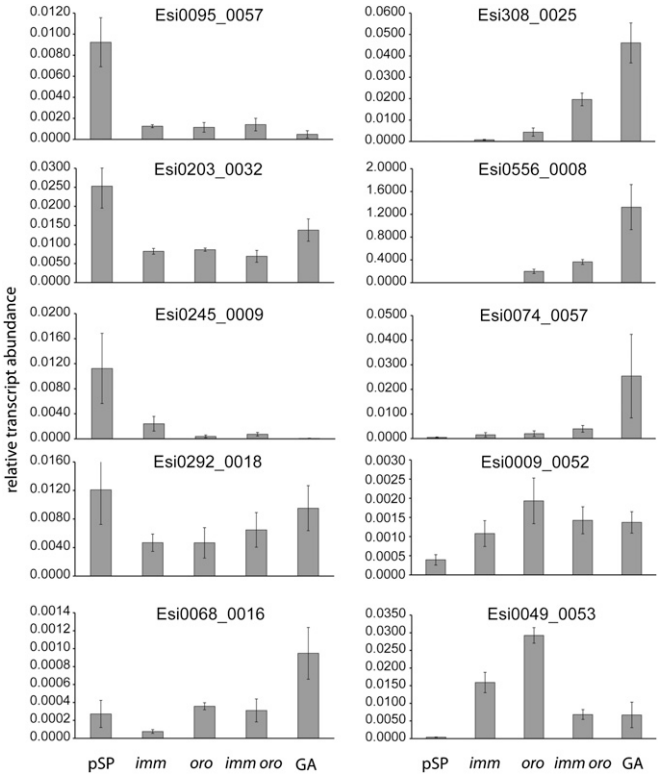

Fig. 5. qRT-PCR analysis of the abundance of gene transcripts in wild-type partheno-sporophyte, *imm, oro, imm oro*, and wild-type gametophytes. Genes were selected either from the microarray analysis or based on their predicted function (see text for details). Data are means of three independent biological replicates ± SE.

Discussion

Mutation at the *ORO* Locus Results in Conversion of the Sporophyte Generation into a Functional Gametophyte. *oro* parthenotes exhibited several features typical of young wild-type gametophytes, including an asymmetric first cell division, production of highly ramified filaments composed exclusively of cylindrical cells, production of sexual structures resembling plurilocular gametangia, positive staining with Congo red, the presence of transcripts of genes that are normally expressed during the gametophyte generation, and production of functional gametes (Fig. 1 and Fig. S2). Together, these results indicate that parthenotes derived from *oro* gametes take on a gametophyte fate and that *ORO* functions either to activate the sporophyte program at the appropriate stage of the life cycle or to repress the gametophyte developmental program during the sporophyte generation. Transcriptomic analysis indicated that the switch from the gametophyte to the sporophyte generation involved predominantly gene repression, providing support for the latter hypothesis.

The global, organism-level developmental modification observed in the *oro* mutant indicates that this gene is a master regulator, influencing a broad range of processes associated with the gametophyte developmental program. This hypothesis was supported by the microarray analysis, which identified a significant number of genes whose transcript abundances were modified in the absence of a functional *ORO* locus.

Interactions Between the *ORO* and *IMM* Loci. The *imm* mutation results in partial conversion of the sporophyte into a gametophyte (18), whereas individuals carrying the *oro* mutation are functional gametophytes that are almost indistinguishable from wild-type gametophytes. The phenotype of the *imm oro* double mutant closely resembled that of the *oro* mutant alone, indicating that *ORO* is at least partially epistatic to *IMM*. There was partial overlap between the sets of genes that exhibited significant changes in transcript abundance compared with the wild-type sporophyte reference for the *imm* and *oro* mutants (16% and 37% of the gene sets for each mutant, respectively), consistent with a partial epistatic relationship between the two genes. Like *oro*, the *imm* mutation resulted in modifications of the transcript abundances of a large number of genes, suggesting that both genes control the expression of many downstream genes (ref. 18 and this study). However, a proportion of the genes that exhibited significant changes in transcript abundance in the wild-type gametophyte compared with the wild-type sporophyte were not represented in the gene lists for the *imm* and *oro* single mutants and the *imm oro* double mutant (70%, 68%, and 56%, respectively), suggesting that even the *imm oro* double mutant does not completely recapitulate the gametophyte developmental program.

***oro* Mutation and Life Cycle Variability.** The isolation of the *oro* mutant has allowed previous observations about the *Ectocarpus*

life cycle and sexuality to be independently confirmed. For example, several lines of evidence indicated that life cycle generation can be uncoupled from ploidy. Haploid, diploid, or tetraploid partheno-sporophytes (25, 26) and haploid, diploid, and aneuploid gametophytes (26–28) have been observed in culture. Here we have shown that zygotes derived from a cross between male and female *oro* mutants give rise to functional, diploid gametophytes. Moreover, crosses carried out using this strain and male and female tester lines indicated that the male haplotype of the sex locus was dominant over the female haplotype. Again, this finding confirms Müller's earlier work on sexually heterozygous gametophytes constructed through laboratory crosses of non-mutant strains (27, 28).

In some species of brown algae, gametes develop parthenogenetically to produce partheno-gametophytes rather than partheno-sporophytes (e.g., *Myriotrichia clavaeformis*; ref. 29). Hence, the modified life cycle observed in individuals carrying the *oro* mutation is the "normal" situation for some brown algal species. However, unlike in the *oro* mutant, their zygotes always develop into sporophytes. Once the genetic lesion that corresponds to the *oro* mutation has been identified, it will be interesting to compare the structure of this locus in species that produce either partheno-sporophytes or partheno-gametophytes.

Changes in life cycle structure have been associated with several important transitions during evolution. In land plants, for example, adaptation to the terrestrial environment appears to have been linked with increasing dominance of the sporophytic stage of the life cycle. The brown algae include organisms with remarkably varied life cycles, ranging from isomorphic, haploid–diploid cycles to diploid cycles in which there is only one multicellular generation. They therefore represent an ideal group both for understanding the adaptive benefits of particular life cycle structures and for investigating the general role played by life cycle modifications in evolutionary processes.

Materials and Methods

Biological Material. Cultivation, crossing, raising of sporophytes from zygotes, isolation of meiotic families, and sexing of gametophyte strains were carried out as described (20, 30). See *SI Materials and Methods* and Table S6 for details.

UV Mutagenesis. Gametes from Ec 32m strain were irradiated with a UV (254 nm) lamp for 45 min immediately after release from plurilocular gametangia. Irradiated gametes were allowed to settle in the dark at 13 °C for 4 h. Petri dishes were then transferred to a culture chamber at 13 °C and cultivated as described above.

Microarray Analysis of mRNA Abundances. Preparation of material, hybridization, and analysis of microarray data were performed essentially as described by Dittami et al. (21). Lists of genes with significant differences in transcript abundance were established by pairwise analyses using the SAM method (22) in the TIGR MeV package (Version 3.1). See *SI Materials and Methods* for details.

qRT-PCR Analysis of Transcript Abundance. qRT-PCR validation was carried out essentially as described by Peters et al. (18). Transcript abundance was estimated based on the analysis of three biological replicates, normalized against the *EF1α* reference gene. See *SI Materials and Methods* and Table S7 for details.

ACKNOWLEDGMENTS. We thank Delphine Scornet, Guillaume Hatte, and Laurence Dartevelle for technical assistance. This work was supported by Centre National de la Recherche Scientifique, Université Pierre et Marie Curie, Groupement d'Interet Scientifique Génomique Marine, the Interreg program France (Channel)-England (project Marinexus), and Agence Nationale de la Recherche (Project Bi-cycle). A.A. was supported by a European Erasmus Mundus Program Fellowship.

1. Coelho SM, et al. (2007) Complex life cycles of multicellular eukaryotes: New approaches based on the use of model organisms. *Gene* 406:152–170.
2. Thornber CS (2006) Functional properties of the isomorphic biphasic algal life cycle. *Integr Comp Biol* 46:605–614.
3. Bicknell RA, Koltunow AM (2004) Understanding apomixis: Recent advances and remaining conundrums. *Plant Cell* 16(Suppl):S228–S245.
4. Koltunow AM, Grossniklaus U (2003) Apomixis: A developmental perspective. *Annu Rev Plant Biol* 54:547–574.
5. Ozias-Akins P, van Dijk PJ (2007) Mendelian genetics of apomixis in plants. *Annu Rev Genet* 41:509–537.
6. Chaudhury AM, et al. (1997) Fertilization-independent seed development in *Arabidopsis thaliana*. *Proc Natl Acad Sci USA* 94:4223–4228.
7. Guitton AE, et al. (2004) Identification of new members of Fertilisation Independent Seed Polycomb Group pathway involved in the control of seed development in *Arabidopsis thaliana*. *Development* 131:2971–2981.
8. Köhler C, et al. (2003) *Arabidopsis* MSI1 is a component of the MEA/FIE Polycomb group complex and required for seed development. *EMBO J* 22:4804–4814.
9. Ohad N, et al. (1996) A mutation that allows endosperm development without fertilization. *Proc Natl Acad Sci USA* 93:5319–5324.
10. Ohad N, et al. (1999) Mutations in *FIE*, a WD polycomb group gene, allow endosperm development without fertilization. *Plant Cell* 11:407–416.
11. Ebel C, Mariconti L, Gruissem W (2004) Plant retinoblastoma homologues control nuclear proliferation in the female gametophyte. *Nature* 429:776–780.
12. Guitton AE, Berger F (2005) Loss of function of *MULTICOPY SUPPRESSOR OF IRA 1* produces nonviable parthenogenetic embryos in *Arabidopsis*. *Curr Biol* 15:750–754.
13. Okano Y, et al. (2009) A polycomb repressive complex 2 gene regulates apogamy and gives evolutionary insights into early land plant evolution. *Proc Natl Acad Sci USA* 106: 16321–16326.
14. Mosquna A, et al. (2009) Regulation of stem cell maintenance by the Polycomb protein FIE has been conserved during land plant evolution. *Development* 136: 2433–2444.
15. Charrier B, et al. (2008) Development and physiology of the brown alga *Ectocarpus siliculosus*: Two centuries of research. *New Phytol* 177:319–332.
16. Cock JM, et al. (2010) The *Ectocarpus* genome and the independent evolution of multicellularity in brown algae. *Nature* 465:617–621.
17. Cock JM, Coelho SM, Brownlee C, Taylor AR (2010) The *Ectocarpus* genome sequence: insights into brown algal biology and the evolutionary diversity of the eukaryotes. *New Phytol* 188:1–4.
18. Peters AF, et al. (2008) Life-cycle-generation-specific developmental processes are modified in the immediate upright mutant of the brown alga *Ectocarpus siliculosus*. *Development* 135:1503–1512.
19. Yamagishi T, Hishinuma T, Kataoka H (2004) Novel sporophyte-like plants are regenerated from protoplasts fused between sporophytic and gametophytic protoplasts of *Bryopsis plumosa*. *Planta* 219:253–260.
20. Peters AF, et al. (2010) Genetic diversity of *Ectocarpus* (Ectocarpales, Phaeophyceae) in Peru and northern Chile, the area of origin of the genome-sequenced strain. *New Phytol* 188:30–41.
21. Dittami SM, et al. (2009) Global expression analysis of the brown alga *Ectocarpus siliculosus* (Phaeophyceae) reveals large-scale reprogramming of the transcriptome in response to abiotic stress. *Genome Biol* 10:R66.
22. Tusher VG, Tibshirani R, Chu G (2001) Significance analysis of microarrays applied to the ionizing radiation response. *Proc Natl Acad Sci USA* 98:5116–5121.
23. Wuest SE, et al. (2010) *Arabidopsis* female gametophyte gene expression map reveals similarities between plant and animal gametes. *Curr Biol* 20:506–512.
24. Khurana JS, Theurkauf W (2010) piRNAs, transposon silencing, and *Drosophila* germline development. *J Cell Biol* 191:905–913.
25. Bothwell JH, Marie D, Peters AF, Cock JM, Coelho SM (2010) Role of endoreduplication and apomeiosis during parthenogenetic reproduction in the model brown alga *Ectocarpus*. *New Phytol* 188:111–121.
26. Müller DG (1967) Generationswechsel, Kernphasenwechsel und Sexualität der Braunalge *Ectocarpus siliculosus* im Kulturversuch. *Planta* 75:39–54.
27. Müller DG (1975) Sex expression in aneuploid gametophytes of the brown alga *Ectocarpus siliculosus* (Dillw.) Lyngb. *Arch. Protistenk. Bd* 117:297–302.
28. Müller DG (1970) Diploide, heterozygote gametophyten bei der braunalge *Ectocarpus siliculosus*. *Naturwissenschaften* 57:357–358.
29. Peters AF, Marie D, Scornet D, Kloareg B, Cock JM (2004) Proposal of *Ectocarpus siliculosus* (Ectocarpales, Phaeophyceae) as a model organism for brown algal genetics and genomics. *J Phycol* 40:1079–1088.
30. Peters AF, Scornet D, Müller DG, Kloareg B, Cock JM (2004) Inheritance of organelles in artificial hybrids of the isogamous multicellular chromist alga *Ectocarpus siliculosus* (Phaeophyceae). *Eur J Phycol* 39:235–242.

Supporting Information

Coelho et al. 10.1073/pnas.1102274108

SI Materials and Methods

Biological Material. Three of the *Ectocarpus* strains used in this study were offspring of a field sporophyte collected in 1988 in San Juan de Marcona, Peru (Ec 17). These strains were Ec 32 (wild-type male), Ec 25 (wild-type female), and Ec 137 (male individual carrying the spontaneous *immediate upright* mutation; ref. 1). Ec 32 is the strain for which a complete genome sequence is available (2). The *immediate upright* mutation was introgressed into a female background by crossing with Ec 25 and isolating meiotic offspring from the resulting sporophyte Ec 372 (1). The female *imm* strain was designated Ec 419. The *ouroboros* mutant strain (Ec 494) was produced by UV mutagenesis of strain Ec 32 (see below). Ec 494 was back-crossed with Ec 25, resulting in sporophytes heterozygous for *oro*, which in turn produced a generation of gametophytes that carried *oro.* These gametophytes should have had a reduced level of any additional substitutions introduced during the mutagenesis. These gametophytes were either female (e.g., Ec 560) or male. One of the male strains (Ec 561) was used for a cross with a genetically more distantly related female strain [Ec 568, meiotic offspring of a field sporophyte (Ec 721) from Arica, northern Chile (3)]. Note that offspring derived by asexual, clonal propagation (e.g., via mitospores or parthenogenetic regeneration of gametes) were considered to be identical to their parents and retained the same strain number. For further details, see Table S6.

Cultivation, crossing, raising of sporophytes from zygotes, isolation of meiotic families, and sexing of gametophyte strains were carried out as described (3, 4). Day length was 10-h light: 14-h dark. For the study of germination, spores or gametes were allowed to settle on coverslips. Zygotes were produced and isolated as described by Peters et al. (4). The sex of gametophytes was determined by microscopic observation of zygote formation in hanging-drop preparations (5) in which the strains to be tested had been combined with fertile thalli of male and female reference strains. Genetic analysis of meiotic offspring followed (6).

Photopolarization Tests. Gametophytes and sporophytes were grown at low density in 5-cm (7-8 mL) Petri dishes under unidirectional white light. The orientation of germination was scored ($n > 300$) according to four quadrants (i.e., toward the light, away from the light, or in one of the two quadrants perpendicular to the light). Algae that germinated into the quadrant away from the light were scored as exhibiting negative phototrophy.

Microarray Analysis of mRNA Abundances. The microarray used to evaluate mRNA abundance in wild-type and mutant algae has been described (7). The microarray is based on 17,119 contig and singleton sequences derived from 90,637 EST sequences that have been mapped to 10,600 of the 16,256 genes identified in the *Ectocarpus* genome (2).

To prepare material for the microarray analysis, the *imm* and *oro* mutants were crossed, and one of the resulting diploid sporophytes was used to produce a segregating population of 269 gametophytes. Parthenotes were derived from these gametophytes by gamete germination and were classified into four groups based on morphological phenotype during early development: wild-type, *imm* mutants, *oro* mutants, and *imm oro* double mutants. RNA was extracted in triplicate (three biological replicates) from 12 bulked segregants from each of these groups and from wild-type gametophyte material (Ec 32). The parthenotes were allowed to fully develop vegetatively before harvesting, with many individuals carrying plurilocular zoidangia (i.e., either sporangia or gametangia depending on the life cycle generation). Partheno-sporophytes were harvested before they produced unilocular sporangia. Bulked segregatants were used to minimize variation due to unlinked polymorphic loci that may have been segregating in the population. RNA was extracted from ~300 mg (wet weight) of tissue following a modified version (1) of the protocol described by Apt et al. (8). Briefly, this protocol involved extraction with a cetyltrimethylammonium bromide (CTAB)-based buffer and subsequent phenol-chloroform purification, LiCl-precipitation, and DNase digestion (Turbo DNase, Ambion) steps. RNA quality and concentration was then analyzed on 1.5% agarose gel stained with ethidium bromide and a NanoDrop ND-1000 spectrophotometer (NanoDrop Products).

Double-stranded cDNA was synthesized and amplified with the SMART cDNA synthesis kit (Clontech) and the M-MuLV reverse transcriptase (Finnzymes) starting from 100 ng of total RNA. The PCR amplification was optimized for each sample so that the minimum number of cycles necessary to produce good-quality cDNA (between 19 and 27 depending on the sample) was used. After phenol:chloroform:isoamyl alcohol (25:24:1) extraction and ethanol precipitation, the cDNA was resuspended in 14 μL of water. cDNA samples used for microarray hybridizations were required to fulfill the following quality criteria: concentration > 250 μg l-1, A260/280 ≥ 1.7, A260/230 ≥ 1.5, median size ≥ 400 bp. Hybridizations were carried out as described (7), and statistical analysis was carried out using the Statistical Analysis of Microarrays (SAM) method (9) in the TIGR MeV package (Version 3.1). Gene Ontology (GO) annotation was used to assign genes to functional categories (http://www.geneontology.org). To identify general trends, the GO annotation was converted into GO slim annotation.

To carry out a global cluster analysis, a one-way ANOVA test (with P values adjusted using the Benjamini Hochberg method) was carried out to identify genes that exhibited significant variances in transcript abundance across the five sample classes. The 4,046 genes identified by this test were then grouped into four clusters of 1,352; 1,262; 1,032; and 400 genes using uncentered Pearson correlation distance and Ward linkage. These clusters included 230, 207, 136, and 56 genes with GO annotations, respectively. To identify overrepresented or underrepresented categories of gene function, the GO annotations were converted to GO slim annotations (using GOslim_pir; http://www.geneontology.org/GO.slims.shtml) and, for each cluster, the abundance of each category was compared with its abundance in the genome as a whole.

qRT-PCR Analysis of mRNA Abundances. Total RNA was extracted from three biological replicates of wild-type, *imm* mutant, *oro* mutant, and *oro imm* double mutant parthenotes and from wild-type gametophytes using a protocol adapted from ref. 8. The samples used for qRT-PCR analysis were not the same as those analyzed in the microarray experiment. Contaminating genomic DNA was eliminated by DNase treatment by using the TURBO DNA-free kit (Applied Biosystems). The concentration and quality of the RNA was determined by spectrophotometry and agarose gel electrophoresis. Between 0.2 and 2.0 μg of total RNA was reverse-transcribed to produce cDNA using the SuperScript First-Strand Synthesis System for RT-PCR (Invitrogen). Real-time qRT-PCR was performed on RNA from pooled samples (10 different strains for each phenotype, in triplicate).

Primer pairs were designed using the Primer3 software (http://frodo.wi.mit.edu/primer3/) so that the amplified fragment corresponded to the 3′UTR region or the most 3′ exon of the gene

being analyzed (Table S7). Primer parameters were as follows: amplicon size 80–180 bp, primer length between 18 and 24 nucleotides (optimum 20 nucleotides), Tm between 59 °C and 61 °C (optimum 60 °C), %GC between 30% and 70% (optimum 50%). The specificity of the primers was tested both by comparing with the *Ectocarpus* genome and cDNA database sequence using Blast and by carrying out *in silico* PCR simulations using the e-PCR program (10).

qRT-PCR was carried out using the ABsolute QPCR SYBR Green ROX Mix (ThermoScientific) in a Chromo4 thermocycler (Bio-Rad Laboratories), and data were analyzed with the Opticon monitor 3 software (Bio-Rad Laboratories). The specificity of amplification was checked using a dissociation curve. The amplification efficiency was tested using a genomic dilution series and was always between 90% and 110%. To allow quantification, a standard curve was established for each gene by using a range of dilutions of *Ectocarpus* genomic DNA (between 80 and 199,600 copies), and expression level was normalized against the *EF1α* reference gene (11). Two technical replicates were carried out for the standard curves and three technical replicates for the samples. The data shown correspond to mean ± SE for three biological replicates.

1. Peters AF, et al. (2008) Life-cycle-generation-specific developmental processes are modified in the *immediate upright* mutant of the brown alga *Ectocarpus siliculosus*. *Development* 135:1503–1512.
2. Cock JM, et al. (2010) The *Ectocarpus* genome and the independent evolution of multicellularity in brown algae. *Nature* 465:617–621.
3. Peters AF, et al. (2010) Genetic diversity of *Ectocarpus* (Ectocarpales, Phaeophyceae) in Peru and northern Chile, the area of origin of the genome-sequenced strain. *New Phytol* 188:30–41.
4. Peters AF, Scornet D, Müller DG, Kloareg B, Cock JM (2004) Inheritance of organelles in artificial hybrids of the isogamous multicellular chromist alga *Ectocarpus siliculosus* (Phaeophyceae). *Eur J Phycol* 39:235–242.
5. Kawai H, Motomura T, Okuda K (2005) Isolation and purification techniques for macroalgae. *Algal Culture Techniques*, ed Anderson RA (Elsevier, Amsterdam), pp 133–143.
6. Müller DG (1991) Mendelian segregation of a virus genome during host meiosis in the marine brown alga *Ectocarpus siliculosus*. *J Plant Physiol* 137:739–743.
7. Dittami SM, et al. (2009) Global expression analysis of the brown alga *Ectocarpus siliculosus* (Phaeophyceae) reveals large-scale reprogramming of the transcriptome in response to abiotic stress. *Genome Biol* 10:R66.
8. Apt KE, Clendennen SK, Powers DA, Grossman AR (1995) The gene family encoding the fucoxanthin chlorophyll proteins from the brown alga *Macrocystis pyrifera*. *Mol Gen Genet* 246:455–464.
9. Tusher VG, Tibshirani R, Chu G (2001) Significance analysis of microarrays applied to the ionizing radiation response. *Proc Natl Acad Sci USA* 98:5116–5121.
10. Schuler GD (1997) Sequence mapping by electronic PCR. *Genome Res* 7:541–550.
11. Le Bail A, et al. (2008) Normalisation genes for expression analyses in the brown alga model *Ectocarpus siliculosus*. *BMC Mol Biol* 9:75.

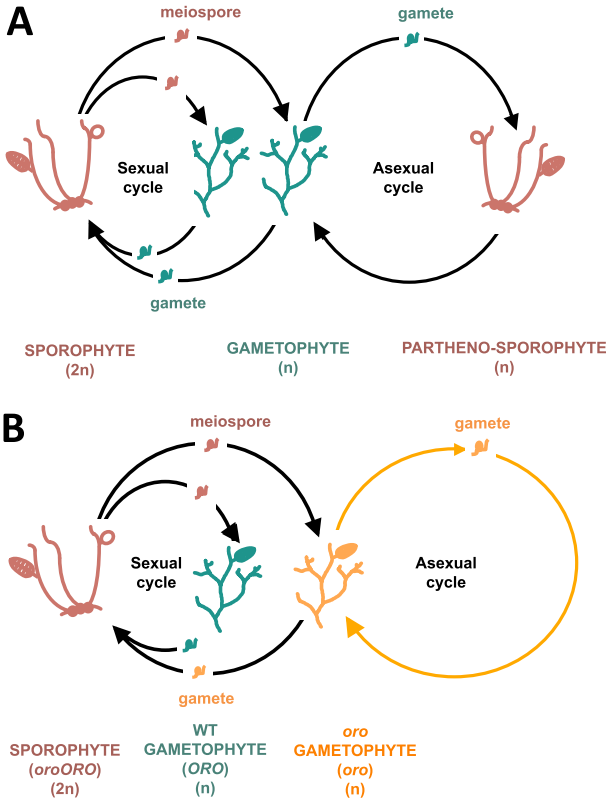

Fig. S1. Comparison of life cycle transitions in wild-type *Ectocarpus* (*A*) and in the *oro* mutant (*B*).

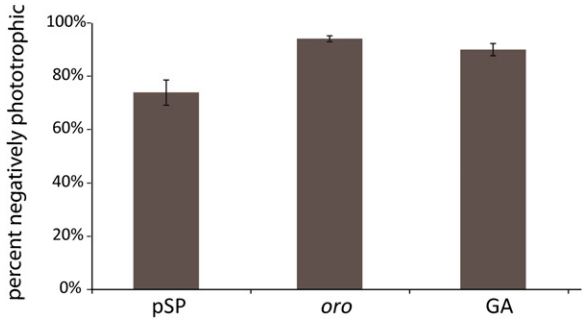

Fig. S2. Photopolarization of *oro* and wild-type *Ectocarpus* germlings in response to unidirectional light. The negative phototropic responses of wild-type gametophytes and of *oro* parthenotes were significantly more marked that those of the wild-type sporophytes. No significant difference was found between the responses of *oro* and wild-type gametophytes. pSP, wild-type partheno-sporophyte; GA, wild-type gametophyte. Error bars show SDs.

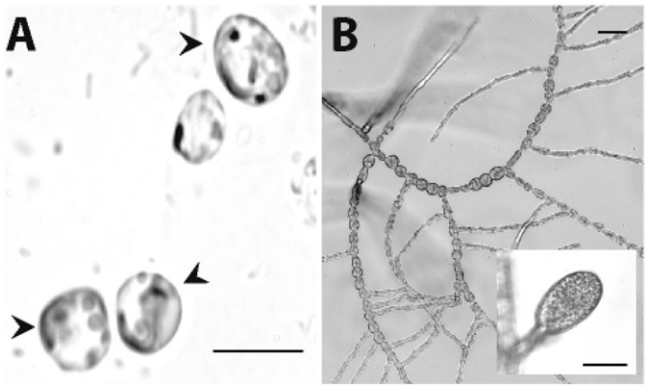

Fig. S3. Sporophyte produced by crossing an *oro* and a wild-type strain. (*A*) Fusion of gametes produces zygotes (arrowheads). (*B*) Zygotes grow into diploid sporophytes, which develop unilocular sporangia (*Inset*) where meiosis takes place. (Scale bars: 10 μm.)

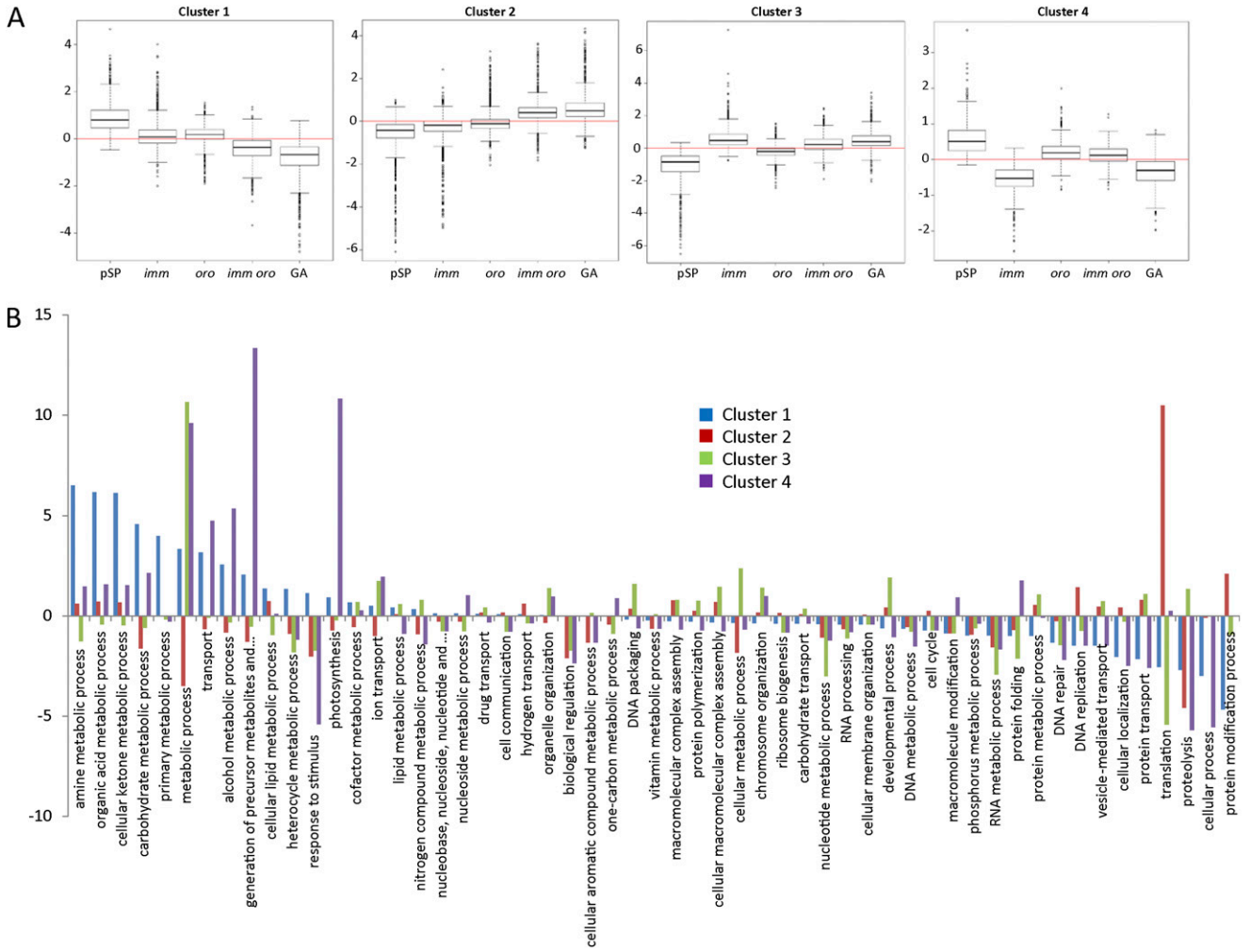

Fig. S4. Cluster analysis of the data from the microarray analysis of transcript abundance in sporophyte, gametophyte, and mutant individuals. (*A*) Box plots showing the trends in transcript abundance for four clusters of genes that had been identified as being differentially expressed by ANOVA test (see *SI Materials and Methods*). Clusters 1–4 contain 1,352, 1,262, 1,032, and 400 genes, respectively. Log2 transcript abundances for each gene are presented as the hybridization signal divided by a reference value corresponding to the median hybridization signal for that gene across all of the samples analyzed. (*B*) Percentage abundance of genes with specific GO slim assignments within each cluster relative to the abundance of genes with the same GO slim assignment in the genome as a whole. Only GO slim categories that represent at least 0.3% of the total in the genome as a whole are shown. pSP, wild-type partheno-sporophyte; GA, wild-type gametophyte.

Table S1. Phenotypic analysis of families of gametophytes derived from individual unilocular sporangia from sporophytes heterozygous at the *ORO* locus

Unilocular sporangium	No, of individuals*	No. of wild-type individuals	No. of *oro* individuals
1	24	10	14
2	25	13	12
3	26	10	16
4	24	11	13
5	25	13	12
6	26	15	11
7	19	11	8
8	25	8	17
9	22	5	17
10	21	13	8
11	25	14	11
12	25	13	12
13	25	12	13
14	27	14	13
Total	339	162	177

*Number of individuals scored per unilocular sporangium.

Table S2. Determination of the sex of families of *oro* gametophytes derived from individual unilocular sporangia from sporophytes heterozygous at the *ORO* locus

Unilocular sporangium	No, of *oro* females	No. of *oro* males
1	3	4
2	1	6
3	3	5
4	4	2
5	5	2
6	1	4
7	5	4
8	4	7
9	3	4
10	0	3
11	2	1
12	2	6
Total	33	48

Table S3. Phenotypic analysis of families of gametophytes derived from individual unilocular sporangia from sporophytes heterozygous for both the *oro* and *imm* mutations

Unilocular sporangium	No. of WT individuals	No. of *oro* individuals	No. of *imm* individuals	No. of *oro imm* individuals
1	6	8	1	1
2	8	2	0	10
3	2	3	1	3
4	9	6	1	4
5	4	8	4	0
6	6	3	3	7
7	4	6	5	5
8	4	7	2	5
9	1	8	10	0
10	9	3	8	0
11	4	6	2	6
12	1	3	5	10
13	5	4	5	6
14	3	3	4	7
15	4	3	2	4
16	4	2	2	7
Total	75	76	60	79

The heterozygous sporophytes were derived by crossing two gametophytes carrying respectively the *imm* and *oro* mutations.

Table S4. Phenotypic analysis of families of gametophytes derived by back-crossing a gametophyte carrying both the *imm* and *oro* mutations with a wild-type strain

Unilocular sporangium	No. of individuals*	No. of *oro* individuals	No. of *imm* individuals	No. of *imm oro* individuals	No. of wild-type individuals
1	21	6	5	6	4
2	16	5	3	3	5
3	16	3	3	4	6
4	14	6	2	3	3
5	26	9	3	9	5
6	17	3	3	5	6
7	16	5	6	2	3
Total	126	37	25	32	32

*Number of individuals scored per unilocular sporangium.

Table S5. Fold differences in transcript abundance relative to the wild-type sporophyte, as measured by qRT-PCR

Locus ID	Predicted function	Fold change expression (log2)			
		imm/pSP	*oro*/pSP	*imm oro*/pSP	GA/pSP
Esi0009_0052	3′5′-Cyclic nucleotide phosphodiesterase domain	1.76	2.32	1.92	1.97
Esi0049_0053	Adhesin-like protein	5.13**	5.81**	3.88**	3.68**
Esi0068_0016	Swi/SNF domain protein	−1.49	0.41	0.37	2.10
Esi0074_0057	Homeodomain-like	0.01	2.13	2.18*	6.12*
Esi0095_0057	Transcription factor (Myb and SANT domains)	−2.74*	−3.23*	−2.93*	−4.55*
Esi0203_0032	Argonaut	−1.63**	−1.46**	−1.89**	−0.97**
Esi0245_0009	*imm* down-regulated 17	−2.22	−4.82	−3.94	−7.31*
Esi0292_0018	SMAD/FHA domain protein	−1.37	−1.38	−0.90	−0.35
Esi0308_0025	Serine/threonine-protein kinase	4.61**	7.18**	9.36**	10.59**
Esi0556_0008	Putative cell wall structural protein	2.50	10.46**	11.33**	13.20**

Fold changes, calculated using log2 values, are the average of three independent biological replicates. Significant differences (ANOVA) with respect to transcript abundance in wild-type sporophytes are indicated. *$P < 0.05$; **$P < 0.01$. GA, wild-type gametophyte; *imm*, imm mutant; *oro*, oro mutant; pSP, wild-type partheno-sporophyte.

Table S6. *Ectocarpus* strains used in this study

Name	Generation, sex	Life history phenotype	Genotype	Description	Origin	Year	CCAP strain code
Ec17	SP	Wild type	*ORO ORO*	Field isolate	San Juan de Marcona, Peru	1988	CCAP 1310/193
Ec25	GA f	Wild type	*ORO*	Meiotic offspring from Ec17	Laboratory	2002	CCAP 1310/3
Ec32	GA m	Wild type	*ORO*	Meiotic offspring from Ec17	Laboratory	2002	CCAP 1310/4
Ec137	GA m	*imm*	*imm*	Meiotic offspring from Ec17, carrying imm mutation	Laboratory	2002	CCAP 1310/319
Ec197	SP	Wild type	*imm IMM oro ORO*	Cross 597f imm+oro x 32m	Laboratory, this work	2009	
Ec372	SP	Wild type	*IMM imm*	Cross 25f wt x 137m imm	Laboratory	2003	CCAP 1310/320
Ec400	GA m	no data	No data	Male reference strain for sex test by crossing	Laboratory	2002	CCAP 1310/329
Ec410	GA f	no data	No data	Female reference strain for sex test by crossing	Laboratory	2002	CCAP 1310/330
Ec419	GA f	*imm*	*imm ORO*	Female gametophyte carrying the *imm* mutation, wild type for *oro*	Laboratory	2003	CCAP1310/321
Ec494	GA m	*oro*	*oro*	UV-mutagenized Ec32, life-history mutant *"ouroboros"*	Laboratory, this work	2005	
Ec568	GA f	Wild type	*ORO*	Meiotic offspring from Ec721	Laboratory	2006	CCAP 1310/334
Ec555	SP	Wild type	*ORO oro*	Cross 25f wt x 494m oro	Laboratory, this work	2005	
Ec556	SP	Wild type	*ORO oro*	Cross 25f wt x 494m oro	Laboratory, this work	2005	
Ec557	SP	Wild type	*ORO oro*	Cross 25f wt x 494m oro	Laboratory, this work	2005	
Ec560	GA f	*oro*	*oro*	Meiotic offspring from Ec557	Laboratory, this work	2005	
Ec561	GA m	*oro*	*oro*	Meiotic offspring from Ec556	Laboratory, this work	2005	
Ec702	SP	Wild type	*ORO oro*	Cross 568f wt x 561m oro	Laboratory, this work	2007	
Ec566	SP	Wild type	*imm IMM oro ORO*	Cross 419f imm x 494m oro	Laboratory, this work	2006	
Ec581-9	GA m	oro	*oro oro*	Cross of 560f o x 494m o	Laboratory, this work	2006	
Ec592	GA	Wild type	*IMM ORO*	Meiotic offspring from 566	Laboratory, this work	2007	
Ec594	GA	*imm*	*imm ORO*	Meiotic offspring from 566	Laboratory, this work	2007	
Ec597	GA f	*imm oro*	*imm oro*	Meiotic offspring from 566	Laboratory, this work	2007	
Ec600	GA	oro	*IMM oro*	Meiotic offspring from 566	Laboratory, this work	2007	
Ec721	SP	Wild type	*ORO ORO*	Field isolate	Arica, Chile	2006	

CCAP, Culture Collections of Algae and Protozoa (marine) reference number, Dunstaffnage Marine Laboratory, Oban, Scotland; GA, gametophyte; *imm*, *immediate upright* mutation; *oro*, *ouroboros* mutation; SP, sporophyte.

Table S7. Oligonucleotides used for the qRT-PCR analysis

Locus_ID	Sequence	Amplicon size, bp
Esi0009_0052		
3′UTR	AAGCGGGTTTACCGAGTGTT	149
3′UTR	GCGCCTCCATTTCTTTCTCT	
Esi0010_0199		
Last exon	AGGAGAAGACGGCACGATT	92
Last exon	GGCCATTCCCAAAGTCCT	
Esi0049_0053		
3′UTR	ATCGTGTTCAGTCGGATGG	139
3′UTR	GAGCAGTCTCAGGACCAACAA	
Esi0068_0016		
Exon 4	CTCCCGGAAACAACAATGAA	95
Exon 4	GTCTGACCGCGCTTGATAAC	
Esi0074_0057		
3′UTR	GGGTTAAAGGGACAGCAACA	125
3′UTR	CAGCGAGGGAGGTGATTAGA	
Esi0095_0057		
3′UTR	ATCAGGCTGAGGTGGTGTTT	111
3′UTR	ACCCGGAATATCGACAGGTT	
Esi0138_0012		
3′UTR	CAGCTACGTGTCGATCTTGG	121
3′UTR	GATGGATGTCAGAGAGGCAGA	
Esi0203_0032		
3′UTR	GCCGATGTCTGTCTTGTTTG	141
3′UTR	TCTAGCCTGCCTGTTCGTTT	
Esi0245_0009		
3′UTR	GAACAACGACCTCCGTAACC	132
3′UTR	GCCGCAACCATGAAGTAATC	
Esi0292_0018		
3′UTR	AGCCTTGTTTGGTACGTGGA	110
3′UTR	CAACCCGCCAAAGATAGATG	
Esi0308_0025		
Last exon	CTCAACCAAGGCTGTGACC	132
3′UTR	CGGTTCCTCATCTTGGTACTCT	
Esi0445_0006		
3′UTR	GATGGCGGGAACTACAACA	134
3′UTR	CAACAGACCGCACCAAATAC	
Esi0556_0008		
3′UTR	GTATCTGGCGACTGGATGCT	101
3′UTR	CGACGGAAACCCAGGTAAA	
Esi0387_0021 (EsEF1α)		
Last exon	CAAGTCCGTCGAGAAGAAGG	147
3′UTR	CCAGCAACACCACAATGTCT	

Locus_ID, *Ectocarpus* gene model.

Other Supporting Information Files

Dataset S1 (XLSX)